


Effect of angular momentum transfer on the angular distribution of Auger electrons following atomic inner ns^2 -shell photoionization

L. Gerchikov **Department of Experimental Physics, Peter the Great St. Petersburg Polytechnic University, 195251 St. Petersburg, Russia*S. Sheinerman †*Department of Physics, St. Petersburg State Marine Technical University, 190121 St. Petersburg, Russia*

(Received 22 December 2020; accepted 22 February 2021; published 5 March 2021)

A mechanism of angular-momentum transfer between photoelectrons and Auger electrons is applied to Auger electron emission in process of photoionization of deep inner atomic shells followed by Auger decay. This mechanism proves to be the leading contribution to distortion of angular distribution of the Auger electrons and highlights important features of postcollision interaction effect in the inner shells photoionization. The theory developed is applied to the photoionization of ns^2 shells of noble gases. Calculations show the noticeable influence of angular-momentum transfer on the Auger-electron angular distribution in a number of cases. Photoionization processes suitable for experimental observation of the proposed effect are discussed.

DOI: [10.1103/PhysRevA.103.032807](https://doi.org/10.1103/PhysRevA.103.032807)

I. INTRODUCTION

Inner atomic shell photoionization leads to creation of inner-shell vacancy and emission of photoelectron. A radiationless decay of created vacancy occurs in the easiest case through Auger decay with an emission of Auger electrons. In the final state of process under consideration, three particles, the photoelectron, the Auger electron, and the doubly charged ion, interact each with other by means of Coulomb forces. Such kinds of interaction as well as the interaction of the photoelectron with the singly charged ion in the intermediate state is known as a postcollision interaction (PCI). The PCI leads to distortion of the energy distributions of the emitted photoelectron and Auger electron, which has been widely investigated during the last fifty years (see, e.g., reviews [1,2] and more recent works [3–10]). The PCI distortion of the energy distributions being considered in the near-threshold region implies that the slow photoelectron loses the energy and the fast Auger electron gains the energy. This effect has been described by different theoretical models [11–18] and observed in measurements (see, e.g., Ref. [19]).

Apart from the energy exchange, the PCI can lead to an exchange of the angular momentum between the emitted particles. This effect has not been taken into account by the theoretical models mentioned above and manifests itself in the variation of angular distribution of the emitted photoelectrons. The distortion of the photoelectron angular distribution due to the angular-momentum transfer (AMT) has recently been predicted theoretically [20,21] and has been experimentally verified [22] for the case of near-threshold Ar $1s^2$ -shell photoionization. It has been shown [20] for the case of inner

ns^2 -subshell ionization that the main contribution to AMT comes from the angular-momentum exchange between the slow photoelectron and the fast Auger electron. An angular-momentum exchange with the receded ion is negligible.

On the other hand, the angular-momentum exchange between the photoelectron and the Auger electron should affect the angular distribution of the Auger electrons, too, which has not been investigated earlier either theoretically or experimentally. To distinguish the AMT-related distortion of the Auger-electron angular distribution we consider in this paper the inner ns^2 -subshell photoionization. Without the PCI between the photoelectron and the Auger electron, the angular distribution of the Auger emission resulting from the ns -vacancy decay will be isotropic. Hence, possible anisotropy of the Auger emission should be solely ascribed to the AMT effect.

The proposed mechanism of PCI distortion of the Auger-electron angular distribution should be distinguished from the widely investigated angular distribution of the Auger emission in the resonant Auger transitions [23]. In the latter case, photoexcitation of the core electron occurs to some discrete state while, in our case, the core electron is ionized by the photon and leaves the atom. After resonant photoexcitation, the inner-shell vacancy created decays via a single (SA) or double (DA) Auger transition. The angular distribution of the Auger electrons emitted in SA decay was first studied in Refs. [24,25]. At the same time, an investigation of the angular distributions of the Auger electrons emitted in DA resonant processes has revealed an essential role of angular correlations between the Auger electrons. Such a correlation has been intensively investigated over last 20 years both theoretically [26–29] and experimentally (see, for example, Refs. [30–33]).

Anisotropy of the Auger electrons following the resonant photoexcitation is explained by the fact that the resonant state excited by a linearly polarized light is aligned along the

*lgerchikov@mail.ru

†sergei.sheinerman@gmail.com

photon polarization vector. The alignment leads to an anisotropy of the emitted resonant Auger electrons. Moreover, in the cascade DA processes the alignment is partly transferred to the intermediate ionic state populated in the first decay. Hence, the second-step Auger electrons show also an anisotropic behavior. In both cases the anisotropy of Auger emission is connected with anisotropy of the target atom caused by the polarized light photoexcitation.

On the contrary, in the process considered here of ns^2 -shell photoionization by linear polarized light, the created photoelectron takes away the photon angular momentum, leaving the ion in spherically symmetric state. The anisotropy of Auger emission is not caused by interaction with the ion aligned along the photon polarization vector but results from the PCI with the outgoing photoelectron. The angular-momentum exchange between emitted electrons as a PCI process takes place at larger distances from the target atom, which also differs from the case of the resonant Auger transitions. Thus, the proposed mechanism of AMT is quite different from what has been studied before. To highlight its main features we consider the near-threshold photoionization of the inner ns^2 subshell of the atom. By doing that, we eliminate an alignment of the inner ns vacancy which is created after the slow-photoelectron emission. Then the anisotropy of the Auger electron which is created in the SA decay of the ns vacancy occurs solely due to the PCI between the slow photoelectron and the fast Auger electron. It gives rise to the possibility of experimental observation of AMT effect by means of Auger emission angular distribution measurements.

The paper is organized as follows: In Sec. II, we develop our theory of AMT [20] for the description of the angular distribution of the Auger emission. In Sec. III we use the approach developed to calculate the asymmetry parameter of Auger emission in $1s^2$ photoionization of Ne and Ar followed by SA decay.

The atomic unit system $|e| = m_e = \hbar = 1$ is used throughout.

II. ANGULAR-MOMENTUM TRANSFER BETWEEN PHOTOELECTRONS AND AUGER ELECTRONS

Deep inner-shell photoionization followed by Auger decay of the atomic inner-shell vacancy is a two-step process that can be represented by the scheme

$$\gamma + A \rightarrow e_{ph}(\varepsilon_0 + i\Gamma/2) + A^{+*} \rightarrow e_{ph}(\mathbf{p}_1) + e_A(\mathbf{p}_2) + A^{2+}. \quad (1)$$

In the first step, the incident linear polarized photon ionizes the ns^2 shell of the target atom, resulting in the creation of a long-living metastable autoionizing state of the A^{+*} ion with autoionization width Γ and slow photoelectron e_{ph} with complex energy $\varepsilon_0 + i\Gamma/2$ (ε_0 is the excess photon energy above the threshold) moving in the field of the singly charged ion. In the second step, the long-living intermediate autoionizing state of the A^{+*} ion decays via the Auger process, resulting in the emission of a fast Auger electron e_A and the shake-off of the photoelectron motion by a sudden change of the ion field from the potential of the A^{+*} ion to the field of the doubly charged ion A^{2+} . The amplitude \mathcal{A} of the two-step process (1) is given by the product of the photoabsorption amplitude M_1

and the amplitude M_2 of the Auger decay of the autoionizing state A^{+*} and subsequent PCI processes [20,34,35]:

$$\mathcal{A} = M_1 \langle \Psi_{\mathbf{p}_1, \mathbf{p}_2} \Phi_{A^{2+}} | \hat{M}_2 | \Psi_{\varepsilon_0 + i\Gamma/2} \Phi_{A^{+*}} \rangle. \quad (2)$$

The photoabsorption amplitude M_1 depends slightly on the photon energy, and below we consider it a constant factor. In contrast, the second factor of amplitude \mathcal{A} has a strong resonant dependence on the energy of the outgoing photoelectron and describes the energy and angular-momentum transfer during the PCI. In Eq. (2), $\Phi_{A^{+*}}$ is the wave function of the long-lived intermediate autoionizing state, and $\Psi_{\varepsilon_0 + i\Gamma/2}$ is the outgoing Coulomb partial wave of photoelectron e_{ph} in the intermediate state of process (1). This function describes the propagation of the photoelectron in the field of the A^{+*} ion. It can be obtained as a solution of the inhomogeneous Schrödinger equation with complex energy $\varepsilon_0 + i\Gamma/2$ [34,36]. The real part of this energy ε_0 is the excess of photon energy above the inner-shell ionization threshold, while its imaginary part is determined by the autoionization width Γ of the inner-shell vacancy. We consider the case where a photoelectron is emitted from the deep ns^2 shell of target atom A and therefore has the angular momentum $l = 1$. The operator of the Auger decay is denoted here by \hat{M}_2 . The wave function of the final state is given by the product of doubly charged ion wave function $\Phi_{A^{2+}}$ and the two-body wave function $\Psi_{\mathbf{p}_1, \mathbf{p}_2}$ of the photoelectron and the Auger electron moving in the field of A^{2+} with momenta \mathbf{p}_1 and \mathbf{p}_2 , respectively.

In our approach [20], the two-body wave function $\Psi_{\mathbf{p}_1, \mathbf{p}_2}$ is considered in the 3C approximation (the so-called BBK function) [37]. This approximation takes into account the interaction between the photoelectron and the Auger electron, as well as their interaction with the ion field, and has the correct asymptotical behavior. Such a two-body function has the form

$$\Psi_{\mathbf{p}_1, \mathbf{p}_2}(\mathbf{r}_1, \mathbf{r}_2) = \Psi_{\mathbf{p}_1}(\mathbf{r}_1) \Psi_{\mathbf{p}_2}(\mathbf{r}_2) \phi(\mathbf{r}_1 - \mathbf{r}_2). \quad (3)$$

where $\Psi_{\mathbf{p}_1}(\mathbf{r}_1)$ and $\Psi_{\mathbf{p}_2}(\mathbf{r}_2)$ are the single-particle Coulomb functions of photoelectron and Auger electron moving in the field of the doubly charged ion, and the function $\phi(\mathbf{r}_1 - \mathbf{r}_2)$ describes their relative motion.

The following approximations are based on the fact that, typically, an Auger electron is very fast, $p_2 \gg 1$. In this case, the wave function of the relative electronic motion ϕ can be written in the eikonal approximation [38]

$$\phi(\mathbf{r}) = \exp\left(i \int_0^\infty \frac{dt}{|\mathbf{r} - \mathbf{v}t|\right)}, \quad (4)$$

where $\mathbf{r} = \mathbf{r}_1 - \mathbf{r}_2$ and $\mathbf{v} = \mathbf{v}_1 - \mathbf{v}_2$ are the vectors of relative position and velocity of the photoelectron and the Auger electron, respectively.

It is important that the Auger decay operator \hat{M}_2 in Eq. (2) acts on the atomic and Auger-electron coordinates and does not effect directly the photoelectron coordinates. The former ones have an atomic spatial scale, $r_2 \approx 1$, while the range of photoelectron coordinates that contribute to the amplitude \mathcal{A} in Eq. (2) is much larger, $r_1 \simeq r = |\mathbf{r}_1 - \mathbf{r}_2| \gg 1$. This fact decouples the integrations over Auger and photoelectron coordinates, and the amplitude \mathcal{A} is reduced to the product of M_1 and M_2 amplitudes and the overlap integral

$$\mathcal{A} = M_1 M_2(\mathbf{p}_2, L, M) \langle \Psi_{\mathbf{p}_1}(\mathbf{r}) \phi(\mathbf{r}) | \Psi_{\varepsilon_0 + i\Gamma/2}(\mathbf{r}) \rangle. \quad (5)$$

Amplitude $M_2(\mathbf{p}_2, L, M)$ of the Auger decay depends on the direction of the Auger emission, angular momentum L , and its projection M of the doubly charged residual ion in the final state. The overlap integral in the obtained amplitude \mathcal{A} also depends on the direction of the Auger electron \mathbf{p}_2 due to dependence of the function ϕ [Eq. (4)] on the relative electron velocity $\mathbf{v} = \mathbf{v}_1 - \mathbf{v}_2$.

However, the angular dependence of $M_2(\mathbf{p}_2, L, M)$ does not lead to the angular dependence of Auger-electron emission if the polarization of the resulting A^{2+} ion is not fixed in the experiment. Indeed, evaluating the cross section, one has to sum the squared amplitude $|\mathcal{A}|^2$ [Eq. (5)] over all angular-momentum states M of the A^{2+} ion. The intermediate ionic state A^{+*} is spherically symmetric. Hence, the Auger electron $e_A(\mathbf{p}_2)$ and the residual ion A^{2+} yield the same angular momentum L with opposite projections $\pm M$. The Auger amplitude depends on M and \mathbf{p}_2 as $M_2(\mathbf{p}_2, L, M) \propto Y_{LM}(\mathbf{p}_2)$. Thus, the sum of $|M_2(\mathbf{p}_2, L, M)|^2$ over M eliminates its dependence on the direction of \mathbf{p}_2 since $\sum_M |Y_{LM}(\mathbf{p}_2)|^2 = (2L + 1)/4\pi$. It means that the possible angular dependence of the Auger-electron emission can arise only from the overlap integral, i.e., it is provided by the PCI solely.

The relative velocity v between the fast Auger electron and the slow photoelectron is close to v_2 and large in magnitude, $v \gg 1$. This fact allows us to expand the exponential function in Eq. (4) in a power series with respect to small parameter $1/v$ and keep the first two terms. In the zeroth approximation $\phi(\mathbf{r}) = 1$, and amplitude \mathcal{A} (5) reduces to the well known expression for the PCI amplitude [34,35]

$$\mathcal{A}^{(0)} = M_1 M_2 \langle \Psi_{\mathbf{p}_1}(\mathbf{r}) | \Psi_{\varepsilon_0 + i\Gamma/2}(\mathbf{r}) \rangle. \quad (6)$$

This approximation neglects the interaction between the slow photoelectron and the fast Auger electron. The PCI distortion is caused by the shake-off process due to the Auger decay, and this approximation does not take into account the angular-momentum transfer. The outgoing photoelectron $e_{ph}(\mathbf{p}_1)$ carries the same angular momentum $l = 1$ as the intermediate photoelectron $e_{ph}(\varepsilon_0 + i\Gamma/2)$. The overlap integral of the photoelectron wave functions $\Psi_{\mathbf{p}_1}$ and $\Psi_{\varepsilon_0 + i\Gamma/2}$ in amplitude [Eq. (6)] does not depend on the direction of the Auger electron and, consequently, in this approximation the double-differential cross section integrated over final states of the photoelectron and residual ion is isotropic with respect to Auger-electron directions. As demonstrated above, the angular dependence of the amplitudes, $\mathcal{A}^{(0)} \propto M_2(\mathbf{p}_2, L, M) \propto Y_{LM}(\mathbf{p}_2)$, goes out in the cross section after the sum of squared amplitude $|\mathcal{A}^{(0)}|^2$ over the residual ion states. Then the evaluation of the double-differential cross section leads to

$$\frac{d^2\sigma^{(0)}}{d\varepsilon_2 d\Omega_2} = \frac{M}{4\pi} \int |Y_{10}(\mathbf{p}_1) R_{\varepsilon_1, \varepsilon_0 1}|^2 d\Omega_1 = \frac{M}{4\pi} |R_{\varepsilon_1, \varepsilon_0 1}|^2, \quad (7)$$

where $\varepsilon_2 = p_2^2/2$ is the Auger-electron energy, M is the numerical factor containing the product of $|M_1 M_2|^2$ that depends smoothly on ε , $R_{\varepsilon_1, \varepsilon_0 1}$ is the overlap integral between the radial parts $\chi(r)$ of the photoelectron wave functions in the intermediate and final states:

$$R_{\varepsilon_1, \varepsilon_0 1} = \int_0^\infty \chi_{\varepsilon_1, l}(r) \chi_{\varepsilon_0 + i\frac{\Gamma}{2}, 1}^{(+)}(r) dr. \quad (8)$$

Functions χ are normalized to $2\pi\delta(\varepsilon' - \varepsilon)$ and have the standing-wave asymptotic

$$\chi_{\varepsilon, l}(r) = \frac{2}{\sqrt{p_1}} \sin\left(p_1 r + \frac{2}{p_1} \ln(2p_1 r) - \frac{\pi l}{2} + \delta_l\right) \quad (9)$$

for an outgoing photoelectron with energy $\varepsilon = p_1^2/2$ and asymptotic of the outgoing partial wave

$$\chi_{\varepsilon_0 + i\frac{\Gamma}{2}, 1}^{(+)}(r) = \frac{1}{\sqrt{p_0}} \exp\left[i\left(p_0 r + \frac{1}{p_0} \ln(2p_0 r) - \frac{\pi}{2} + \delta_1\right)\right], \quad (10)$$

for the intermediate photoelectron with the energy $\varepsilon_0 + i\Gamma/2 = p_0^2/2$.

Angular-momentum transfer can be taken into account within the next approximation with respect to the Coulomb interaction between the photoelectron and the Auger electron, which is equivalent to the first Born approximation. The corresponding amplitude $\mathcal{A}^{(1)}$ is obtained by keeping in expression (5) the second term of the exponential function expansion for ϕ :

$$\mathcal{A}^{(1)} = -iM_1 M_2 \langle \Psi_{\mathbf{p}_1}(\mathbf{r}) | \int_0^\infty \frac{dt}{|\mathbf{r} - \mathbf{v}t|} |\Psi_{\varepsilon_0 + i\Gamma/2}(\mathbf{r}) \rangle. \quad (11)$$

To evaluate the amplitude (11) we use the partial-wave expansion for the outgoing photoelectron wave function and the multipole expansion for the Coulomb potential, as done in Ref. [20]. Then, integration over all coordinates and time in Eq. (11) results in

$$\begin{aligned} \mathcal{A}^{(1)} = & -2\pi i M_1 M_2 \left(\frac{4\pi}{v}\right) \sum_{l, m, l', m'} \frac{e^{-i(\frac{\pi l}{2} - \delta_l)}}{\sqrt{p_1}} Y_{lm}(\mathbf{p}_1) \\ & \times \frac{\langle Y_{lm} | Y_{l'm'} | Y_{10} \rangle Y_{l'm'}^*(\mathbf{v})}{l'(l' + 1)} \int_0^\infty \chi_{\varepsilon, l}(r) \chi_{\varepsilon_0 + i\frac{\Gamma}{2}, 1}^{(+)}(r) dr, \end{aligned} \quad (12)$$

where l, m are the photoelectron angular momentum and its projection; l', m' are the magnitude and projection of the angular momentum transferred from the photoelectron to the Auger electron. At the photoionization threshold where $v_1 \ll v_2 \simeq v$ we can replace in Eq. (12) the relative velocity vector \mathbf{v} by the Auger-electron velocity \mathbf{v}_2 . It will simplify the further calculations. Note here that the amplitude $\mathcal{A}^{(1)}$, contrary to the amplitude $\mathcal{A}^{(0)}$, has additional angular dependence on the Auger-electron direction via spherical harmonics $Y_{l'm'}^*(\mathbf{v}_2)$, where l' is the transferred angular momentum. As demonstrated earlier, the squared Auger amplitude $|M_2(\mathbf{p}_2, L, M)|^2$ after averaging over the final states of the residual ion L, M does not provide any angular dependence of the cross section on the direction of Auger-electron emission. Thus, the cross-section angular dependence is solely provided by the spherical harmonics $Y_{l'm'}^*(\mathbf{v}_2)$ in the amplitude $\mathcal{A}^{(1)}$. It means that the cross-section angular dependence is not connected with the angular momentum of the Auger electron L gained from the ion A^{+*} at the instant of Auger decay but originates from the angular momentum l' transferred to the Auger electron from the photoelectron in the process of their PCI.

The AMT amplitude $\mathcal{A}^{(1)}$ given by Eq. (12) leads to additional contribution to the cross section. The latter is determined by the square of the modulus of the amplitudes

summed: $|\mathcal{A}^{(0)} + \mathcal{A}^{(1)}|^2$. Let us demonstrate that amplitudes $\mathcal{A}^{(0)}$ and $\mathcal{A}^{(1)}$ do not interfere in the cross section integrated over all directions of the photoelectron momentum \mathbf{p}_1 , $\int \Omega_1 |\mathcal{A}^{(0)} + \mathcal{A}^{(1)}|^2 = \int \Omega_1 |\mathcal{A}^{(0)}|^2 + \int \Omega_1 |\mathcal{A}^{(1)}|^2$. The AMT amplitude $\mathcal{A}^{(1)}$ is represented by Eq. (12) as an expansion over photoelectron partial waves. Zeroth-order amplitude $\mathcal{A}^{(0)}$ contains actually the single partial term with photoelectron angular momentum $l_1 = 1$ and its projection $m_1 = 0$. The terms with different values of l_1 and m_1 do not interfere in the cross section because their products vanish under integration over photoelectron directions. Hence we need to check the interference of the two terms only: the amplitude $\mathcal{A}^{(0)}$ and the partial contribution $\mathcal{A}_{10}^{(1)}$ to $\mathcal{A}^{(1)}$ with $l_1 = 1$ and $m_1 = 0$. Comparing Eqs. (6), (7), (11), and (12), one can see that their ratio is a pure imaginary number, $\text{Re}\{\mathcal{A}_{10}^{(1)}/\mathcal{A}^{(0)}\} = 0$. Conse-

quently, $|\mathcal{A}^{(0)} + \mathcal{A}_{10}^{(1)}|^2 = |\mathcal{A}^{(0)}|^2 + |\mathcal{A}_{10}^{(1)}|^2$. Thus, the zeroth- and first-order amplitudes $\mathcal{A}^{(0)}$ and $\mathcal{A}^{(1)}$ do not interfere in the cross section averaged over all directions of photoelectron emission. Moreover, all partial cross-section contributions corresponding to different values of the photoelectron angular momentum l also do not interfere, but terms with different values of the transferred angular momenta l' and l'' do interfere.

Thus, the cross section is given by the sum of the zero-order contribution $\sigma^{(0)}$ (7) and the second-order contribution $\sigma^{(2)}$ of the AMT process. Evaluation of $d^2\sigma^{(2)}/d\varepsilon_2 d\Omega_2$ is similar to those in the Ref. [20], where it is described in detail. Calculations of the angular parts are based on the properties of the spherical harmonics and Clebsch-Gordan coefficients [39] and lead eventually to

$$\begin{aligned} \frac{d^2\sigma^{(2)}}{d\varepsilon_2 d\Omega_2} &= \frac{3M}{4\pi} \left(\frac{1}{v_2}\right)^2 \sum_k P_k(\cos(\theta_2)) C_{10\ 10}^{k0} \sum_{l, l' > 0, l'' > 0} (-1)^{l+l'+l''} |R_{\varepsilon l, \varepsilon_0 1}|^2 \\ &\times \frac{(2l+1)\sqrt{(2l'+1)(2l''+1)}}{l'l''(l'+1)(l''+1)} \begin{Bmatrix} l & l' & 1 \\ k & 1 & l' \end{Bmatrix} C_{l'0\ l''0}^{k0} C_{10\ 10}^{l'0} C_{10\ 10}^{l''0}. \end{aligned} \quad (13)$$

Here, the factor M has the same value as in Eq. (7), l' and l'' denote the possible values of the transferred angular momentum for given values of the final photoelectron angular momentum l and the angular momentum $l_{\text{int}} = 1$ of the intermediate photoelectron state. The overlap integrals $R_{\varepsilon l, \varepsilon_0 1}$ are defined by the expression (8).

Note that, according to the properties of the Clebsch-Gordan coefficient $C_{10\ 10}^{k0}$, index k runs only through two values, $k = 0, 2$. Consequently, the total differential cross section can be written as the sum of the two first Legendre polynomials $P_k(\cos \theta_2)$, $k = 0, 2$:

$$\begin{aligned} \frac{d^2\sigma}{d\varepsilon_2 d\Omega_2} &= \frac{d^2\sigma^{(0)}}{d\varepsilon_2 d\Omega_2} + \frac{d^2\sigma^{(2)}}{d\varepsilon_2 d\Omega_2} \\ &= \frac{1}{4\pi} \frac{d\sigma}{d\varepsilon_2} [1 + \beta(\varepsilon_2) P_2(\cos \theta_2)], \end{aligned} \quad (14)$$

where σ is the total photoionization cross section and θ_2 is the angle between the direction of Auger emission and the photon polarization vector. The coefficient before $P_2(\cos \theta_2)$ is known as the anisotropy parameter and is denoted β [40,41]. In our zeroth-order approximation $\beta = 0$. A nonzero value of β appears in the next approximation which takes into account the AMT effect. Note that the cross-section angular dependence (14) results from averaging over all residual ion states and photoelectron emission directions \mathbf{p}_1 . Since we fix neither the direction of the photoelectron emission nor the polarization of the residual ion, the only predominant direction is the photon polarization vector, so the Auger emission angular distribution is characterized by a single parameter β . Its deviation from zero value $\beta = 0$ indicates the presence of AMT and therefore gives rise to the possibility of its experimental observation.

The differential photoionization cross sections $d\sigma^{(0)}/d\varepsilon_2$ and $d\sigma^{(2)}/d\varepsilon_2$ show the resonance behavior that results

from the properties of the overlap integrals $R_{\varepsilon l, \varepsilon_0 1}$ (8). The overlapping between the radial wave functions of the final, $\chi_{\varepsilon, l}(r)$ and the intermediate $\chi_{\varepsilon_0 + i\frac{\Gamma}{2}, 1}^{(+)}(r)$ photoelectron states is maximal if their momenta coincide. Consequently, the photoelectron resonance energy is close to the energy of the photoelectron intermediate state, $\varepsilon_1 \simeq \varepsilon_0$. It is slightly redshifted by the PCI of photoelectron with residual ion and blueshifted due to the AMT [20]. Correspondingly, the energy distribution of the Auger electron has a resonance peak at $\varepsilon_2 \simeq E(A^{+*}) - E(A^{2+})$.

If we are interested in the angular distribution of the Auger emission averaged over its linewidth, the double-differential cross section (14) should be integrated over the resonance peak:

$$\frac{d\sigma}{d\Omega_2} = \frac{d\sigma^{(0)}}{d\Omega_2} + \frac{d\sigma^{(2)}}{d\Omega_2} = \frac{\sigma}{4\pi} [1 + \bar{\beta} P_2(\cos \theta_2)], \quad (15)$$

where $\bar{\beta}$ is the averaged asymmetry parameter. Overlap integrals $R_{\varepsilon l, \varepsilon_0 1}$ in the double-differential cross sections (7) and (14) have a similar energy dependence. The substantial deviations occur only at high values of transferred angular momentum [20], whose contributions to the cross section are negligible. It allows us to evaluate the single differential cross section (15) assuming that all integrals $\int |R_{\varepsilon l, \varepsilon_0 1}|^2 d\varepsilon$ are equal. Within this approximation, we get the following closed analytical expressions for the cross section and asymmetry parameter:

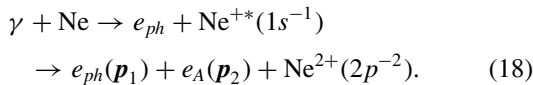
$$\begin{aligned} \sigma &= \sigma^{(0)} + \sigma^{(2)}, \\ \sigma^{(0)} &= M \int |R_{\varepsilon l, \varepsilon_0 1}|^2 d\varepsilon \equiv \sigma_0, \\ \sigma^{(2)} &= \sigma_0 \left(\frac{1}{v_2}\right)^2 \sum_{l>0} \frac{(2l+1)}{l^2(l+1)^2} = \sigma_0 \left(\frac{1}{v_2}\right)^2, \end{aligned} \quad (16)$$

$$\bar{\beta} = \frac{3}{v_2^2} \sum_{l, l' > 0, l'' > 0} (-1)^{l+l'+l''} \frac{(2l+1)\sqrt{(2l'+1)(2l''+1)}}{l'l''(l'+1)(l''+1)} \times \begin{Bmatrix} l & l'' & 1 \\ 2 & 1 & l' \end{Bmatrix} C_{1010}^{20} C_{l'0l''0}^{20} C_{l010}^{l'0} C_{l010}^{l''0}, \quad (17)$$

where the Auger-electron velocity is determined by the Auger transition energy $v_2^2 = 2E_A = 2[E(A^{+*}) - E(A^{2+})]$. In Eq. (16), l denotes transferred angular momentum, i.e., the total second-order AMT cross section $\sigma^{(2)}$ is given by the sum of partial contributions of all transferred momenta $l > 0$. In Eq. (17), l, l', l'' denote the photoelectron angular momentum and all possible values of transferred angular momentum, respectively, like in Eq. (14). Note that the above expressions (16) and (17) represent the first terms of the expansion with respect to the parameter $1/v_2$. In particular, the expression (17) for $\bar{\beta}$ is given by the single lowest-order term of the expansion. In this approximation, $\bar{\beta}$ depends inversely on the Auger transition energy E_A . Numerically, it reads in atomic units $\bar{\beta} \simeq 0.6/E_A$.

III. RESULTS AND DISCUSSION

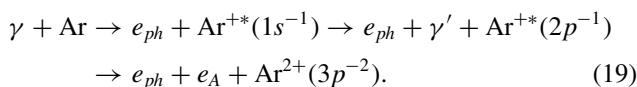
First we apply the developed theory to the experimentally studied photoionization of the Ne $1s^2$ shell followed by the single Auger decay:



The measurements of the β parameter of the angular distribution of the *KLL* Auger electrons emitted in this process were done [42] for the photon energies both below and above the $1s^2$ photoionization threshold. To the best of our knowledge, this is the only case of the β parameter measurements for the Auger electrons following the inner ns^2 shell photoionization.

The energy of the emitted Auger electrons in the process (18) is equal to 800 eV. Our calculations in this case give the anisotropy parameter $\bar{\beta} = 0.02$. This rather low value of $\bar{\beta}$ is caused by large velocity of the emitted Auger electrons ($v_2 \simeq 7.67$ a.u.). That is why experimental resolution of anisotropy parameter measurements in this reaction [42] did not allow us to detect the AMT effect. The reported experimental values of β are close to zero [42], in accord to our calculations.

The Auger decays where the AMT effects could reveal itself occur at smaller velocities of the Auger electrons. Hence, as a second example of an application of the developed theory, we consider the photoionization of the Ar $1s^2$ shell. A direct Auger decay of the $1s^{-1}$ vacancy ($1s^{-1} \rightarrow 3p^{-2} + e_{\text{Auger}}$) occurs with an emission of the Auger electron of large energy ($E_A \simeq 3150$ eV). Akin to the Ne $1s^{-1}$ case, the AMT effect in this decay is also small. Fortunately, this channel of the $1s^{-1}$ vacancy decay has a low probability [43]. The main channel of the decay which leads to the Ar^{2+} ionic state includes the intermediate emission of the 2960 eV photon. So the dominating process of the $1s^2$ photoionization followed by a decay of created vacancy can be presented by the scheme [43]



The AMT-related distortion of the angular distribution of photoelectrons emitted in this process had been predicted in Ref. [20] and recently confirmed experimentally [22]. Here we apply our theory to the Auger-electron angular distribution. The energy of the emitted Auger electron is close to $E_A \simeq 200$ eV.

Note that decay of the $1s^{-1}$ vacancy in Eq. (19) is a cascade process instead of a simpler direct Auger decay considered in our theory. Nevertheless, we demonstrate that the developed theory can be well applied to the process (19), too. If one does not fix the polarization and direction of the emitted photon the Auger emission remains isotropic without PCI between the photoelectron and the Auger electron. Indeed, the angular dependence of the Auger-electron direction goes out from the zero-order cross section of the cascade process after the averaging over the directions and polarization of the emitted photon and over the final states of the residual ion in the same way as it does in Eq. (7). The angular dependence originates from AMT between the photoelectron and the Auger electron in the process of their PCI. For this process the cascade decay just changes the delay time between the creation of the $1s$ vacancy and the Auger-electron emission. It can be described by introduction of the effective decay time $\tau_{\text{eff}} = \tau_{1s} + \tau_{2p}$ and the corresponding effective autoionization width $\Gamma_{\text{eff}} = \Gamma_{1s}\Gamma_{2p}/(\Gamma_{1s} + \Gamma_{2p})$ [7]. In the case of Eq. (19), it gives $\Gamma_{\text{eff}} = 101$ meV.

Calculation of the averaged asymmetry parameter according to Eq. (17) gives the process (19), $\bar{\beta} = 0.08$. It is four times larger than in the case of Ne ionization (18) because the Auger-electron energy in Ar ionization (19) is four times smaller than in Eq. (18). It gives rise to the expectations that AMT-related asymmetry of the Auger emission in the Ar $1s^2$ shell ionization could be experimentally detected.

But the even better candidate for the observation of pronounced AMT-related angular asymmetry of Auger emission is the photoionization of $2s^2$ shell of Ar. The $2s^{-1}$ vacancy can decay by means of the Auger decay $2s^{-1} \rightarrow 2p^{-1}3p^{-1} + e_A$ with an emission of the Auger electron of ≈ 47 eV energy [44]. For this Auger-electron energy, the averaged asymmetry parameter is close to $\bar{\beta} \simeq 0.3$. So an anisotropy of the Auger electrons in this case proves to be rather prominent. An experimental observation of predicted effect is very desirable.

IV. CONCLUSION

The AMT-related distortion of angular distribution of Auger electrons emitted in the inner-shell photoionization has been investigated. In the framework of the quantum-mechanical approach we have demonstrated that the angular-momentum exchange between the Auger electron and the photoelectron leads to the anisotropy of Auger emission. This effect reveals itself in the PCI phenomenon at the photon energies above the inner ns^2 -photoionization threshold. The proposed mechanism of Auger emission anisotropy differs substantively from those in the resonant Auger transition below the photoionization threshold. The anisotropy parameter β of Auger emission has been calculated by using the theory developed for several inner ns^2 -shell ionization processes

accompanied by a single Auger decay. In the case of the Ar ns^2 photoionization, we report the pronounced anisotropy of

Auger emission, which opens an opportunity for experimental observation of the AMT effect.

-
- [1] M. Yu. Kuchiev and S. A. Sheinerman, *Sov. Phys. Usp.* **32**, 569 (1989).
- [2] V. Schmidt, *Rep. Prog. Phys.* **55**, 1483 (1992).
- [3] A. K. Kazansky and N. M. Kabachnik, *Phys. Rev. A* **72**, 052714 (2005).
- [4] A. K. Kazansky and N. M. Kabachnik, *J. Phys. B: At., Mol. Opt. Phys.* **39**, L53 (2006).
- [5] F. Penent, S. Sheinerman, L. Andric *et al.*, *J. Phys. B: At., Mol. Opt. Phys.* **41**, 045002 (2008).
- [6] L. Gerchikov and S. Sheinerman, *Phys. Rev. A* **84**, 022503 (2011).
- [7] R. Guillemin, S. Sheinerman, C. Bomme *et al.*, *Phys. Rev. Lett.* **109**, 013001 (2012).
- [8] S. Sheinerman, P. Linusson, J. H. D. Eland, L. Hedin, E. Andersson, J. E. Rubensson, L. Karlsson, and R. Feifel, *Phys. Rev. A* **86**, 022515 (2012).
- [9] J. Palaudoux, S. Sheinerman, J. Soronen *et al.*, *Phys. Rev. A* **92**, 012510 (2015).
- [10] R. Guillemin, S. Sheinerman, R. Puttner, T. Marchenko, G. Goldsztejn, L. Journel, R. K. Kushawaha, D. Ceolin, M. N. Piancastelli, and M. Simon, *Phys. Rev. A* **92**, 012503 (2015).
- [11] G. C. King, F. H. Read, and R. C. Bradford, *J. Phys. B: At. Mol. Phys.* **8**, 2210 (1975).
- [12] A. Niehaus, *J. Phys. B: At. Mol. Phys.* **10**, 1845 (1977).
- [13] K. Helenelund, S. Hedman, L. Asplund, U. Gelius, and K. Siegbahn, *Phys. Scr.* **27**, 245 (1983).
- [14] G. B. Armen, T. Aberg, J. C. Levin, B. Crasemann, M. H. Chen, G. E. Ice, and G. S. Brown, *Phys. Rev. Lett.* **54**, 1142 (1985).
- [15] S. Hedman, K. Helenelund, L. Asplund, U. Gelius, and K. Siegbahn, *J. Phys. B: At. Mol. Phys.* **15**, L799 (1982).
- [16] M. Yu. Kuchiev and S. A. Sheinerman, *Sov. Phys. JETP* **63**, 986 (1986).
- [17] M. Yu. Kuchiev and S. A. Sheinerman, *J. Phys. B: At., Mol. Opt. Phys.* **21**, 2027 (1988).
- [18] P. van der Straten, R. Morgenstern, and A. Niehaus, *Z. Phys. D: At., Mol. Clusters* **8**, 35 (1988).
- [19] S. Sheinerman, P. Lablanquie, F. Penent *et al.*, *J. Phys. B: At., Mol. Opt. Phys.* **43**, 115001 (2010).
- [20] L. Gerchikov, R. Guillemin, M. Simon, and S. Sheinerman, *Phys. Rev. A* **95**, 063425 (2017).
- [21] L. Gerchikov and S. Sheinerman, *J. Phys. B: At., Mol. Opt. Phys.* **51**, 065201 (2018).
- [22] R. Guillemin *et al.*, *Phys. Rev. A* **99**, 063409 (2019).
- [23] G. B. Armen, H. Aksela, T. Åberg, and S. Aksela, *J. Phys. B: At., Mol. Opt. Phys.* **33**, R49 (2000).
- [24] N. M. Kabachnik and I. P. Sazhina, *J. Phys. B: At. Mol. Phys.* **17**, 1335 (1984).
- [25] V. V. Balashov, A. N. Grum-Grzhimailo, and N. M. Kabachnik, *Polarization and Correlation Phenomena in Atomic Collisions. A Practical Theory Course* (Kluwer Plenum, New York, 2000).
- [26] N. M. Kabachnik, I. P. Sazhina, and K. Ueda, *J. Phys. B: At., Mol. Opt. Phys.* **32**, 1769 (1999).
- [27] M. Ya. Amusia, I. S. Lee, and V. A. Kilin, *Phys. Rev. A* **45**, 4576 (1992).
- [28] J. Tulkki, N. M. Kabachnik, and H. Aksela, *Phys. Rev. A* **48**, 1277 (1993).
- [29] A. N. Grum-Grzhimailo and N. M. Kabachnik, *J. Phys. B: At., Mol. Opt. Phys.* **37**, 1879 (2004).
- [30] K. Ueda *et al.*, *J. Phys. B: At., Mol. Opt. Phys.* **32**, L291 (1999).
- [31] H. Yoshida *et al.*, *J. Phys. B: At., Mol. Opt. Phys.* **33**, 4343 (2000).
- [32] Y. Shimizu *et al.*, *J. Phys. B: At., Mol. Opt. Phys.* **33**, L685 (2000).
- [33] H. Yoshida *et al.*, *J. Phys. B: At., Mol. Opt. Phys.* **38**, 465 (2005).
- [34] M. Yu. Kuchiev and S. A. Sheinerman, *J. Phys. B: At. Mol. Phys.* **18**, L551 (1985).
- [35] S. A. Sheinerman, *J. Phys. B: At., Mol. Opt. Phys.* **36**, 4435 (2003).
- [36] M. Yu. Kuchiev and S. A. Sheinerman, *Comput. Phys. Commun.* **39**, 155 (1986).
- [37] M. Brauner, J. S. Briggs, and H. Klar, *J. Phys. B: At., Mol. Opt. Phys.* **22**, 2265 (1989).
- [38] L. D. Landau and E. M. Lifshitz, *Quantum Mechanics*, 3rd ed. (Butterworth-Heinemann, Amsterdam, 1977), Chap. VI.
- [39] D. A. Varshalovich, A. N. Moskalev, and V. K. Khersonskii, *Quantum Theory of Angular Momentum* (World Scientific, Singapore, 1988).
- [40] D. Dill, A. F. Starace, and S. T. Manson, *Phys. Rev. A* **11**, 1596 (1975).
- [41] S. T. Manson and A. F. Starace, *Rev. Mod. Phys.* **54**, 389 (1982).
- [42] P. H. Kobrin, S. Southworth, C. M. Truesdale, D. W. Lindle, U. Becker, and D. A. Shirley, *Phys. Rev. A* **29**, 194 (1984).
- [43] U. Alkemper, J. Doppelfeld, and F. von Busch, *Phys. Rev. A* **56**, 2741 (1997).
- [44] P. Lablanquie *et al.*, *Phys. Rev. Lett.* **84**, 47 (2000).